Phys. Status Solidi C **12**, No. 12, 1401–1404 (2015) / **DOI** 10.1002/pssc.201510136

physica status solidi pss c
www.pss-c.com
current topics in solid state physics

Optimization of THz response of strained-Si MODFETs

Juan A. Delgado-Notario[1], Yahya M. Meziani[1], J. E. Velázquez-Pérez[*,1], and Kristel Fobelets[,2]**

[1] Departamento de Física Aplicada, Universidad de Salamanca, Pza. de la Merced, 37008 Salamanca, Spain
[2] Department of Electrical and Electronics Engineering, Imperial College, South Kensington Campus, London SW7 2AZ, UK

Received 28 June 2015, accepted 27 July 2015
Published online 31 August 2015

Keywords terahertz, MODFET, SiGe, TCAD, plasma waves

* Corresponding author: e-mail js@usal.es, Phone: + 34 923294436, Fax: + 34 923294584
** e-mail k.fobelets@imperial.ac.uk

This paper reports on the study of strained-Si n-channel MODFETs as detectors of sub-THz radiation. Simulations based on a bi-dimensional hydrodynamic model for the charge transport coupled to a Poisson equation solver were performed. A charge boundary condition for the floating drain contact was implemented to obtain the photovoltaic response of the device. Time-domain simulations were performed to generate the stationary time series needed to obtain the photovoltaic response. A non-resonant THz photo-response was obtained in agreement with experimental results and theoretical works on plasma waves devices. It was found that the photovoltaic response of s-Si MODFETs with non self-aligned gates is strongly influenced by both gate's length and topology. In particular, it was demonstrated that at frequencies around 0.3 THz a double-finger gate delivers a stronger PV response than a conventional single-finger gate structure.

© 2015 WILEY-VCH Verlag GmbH & Co. KGaA, Weinheim

1 Introduction During the past two decades a considerable effort was devoted to the development of Field-Effect Transistors (FETs) using the Si/SiGe material system. N-channel strained-Si FETs with buried [1] (s-Si MODFET, modulation doped FETs) and surface channels [2] (s-Si MOSFET) were developed. Minimum noise figures as low as 0.4 dB at 2.5 GHz and cut-off frequencies (f_T) in excess of 70 GHz at 300 K were achieved in s-Si MODFET [3]. Basic analog building blocks were also demonstrated [4]. Nevertheless, the final break through the market of these technologies was hindered by low-yields of global-strain wafers.

Recently, it has been shown the potential of s-Si MODFETs as room temperature detectors of sub-THz radiation [5, 6], i.e. in frequency ranges far beyond f_T. As Schottky-gated s-Si MODFETs exhibit large values of channel electron mobility (≈2000 $cm^2V^{-1}s^{-1}$ [7]) they can be used as detectors of THz electromagnetic radiation [8]. This has been experimentally demonstrated and the mechanism of detection identified as the excitation of resonant or overdamped plasma waves in the two-dimensional electron plasma in the device channel [6]. The natural substrate compatibility of s-Si MODFETs with conventional Si technologies is a key benefit of the system Si:SiGe to compete in future THz system integration.

2 Device description and models used in simulations In this work, we simulated n-channel s-Si MODFETs. The structure of the simulated device is shown in Fig. 1.

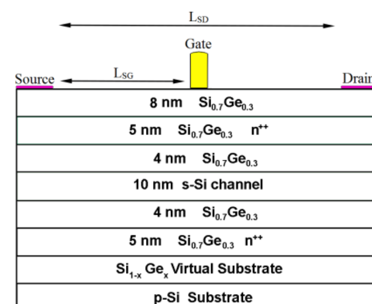

Figure 1 Vertical layout of the s-Si MODFET under study.

Devices had a thick SiGe virtual substrate grown over a p-silicon wafer. The final Ge molar concentration in the

© 2015 WILEY-VCH Verlag GmbH & Co. KGaA, Weinheim

virtual substrate was 0.3. Devices had a 10 nm tensile strained (in terms of biaxial deformation) Si channel, sandwiched between two heavily doped SiGe electron supply layers (doped at ~10^{19} cm^{-3} the top supply layer and ~10^{18} cm^{-3} the bottom one) to generate an electron dual-channel in the strained-Si quantum well.

A set of transistors with different gate lengths (L_G) in the range 50 nm to 500 nm while keeping constant the Source-to-Drain distance (L_{SD}) at 2 µm was studied. The source-to-gate length (L_{SG}) was modified to study the effect of asymmetry in the device by changing the position of the gate.

A 2D numerical study was performed using Synopsys TCAD [9], to understand the response found in THz measurements. Modeling the electrical behavior of transistors with deep-submicron gates needs an accurate description of the complex nature of the carrier transport in the channel. To this aim we used a two-dimensional hydrodynamic (2DHD) self-consistently coupled to a two-dimensional solution of the Poisson equation. In the 2DHD simulations impurity de-ionization, Fermi-Dirac statistics and mobility degradation due to both longitudinal and transverse electric field were taken into account. The source and drain regions were simulated as non-self-aligned implanted contacts.

The study of the THz photovoltaic response of the transistor was implemented, as in measurements [5], by DC biasing source and gate while floating the drain contact. A sub-THz sinusoidal signal was superimposed to the gate voltage as described in [8]. The amplitude of the gate signal was fixed to 5 mV; the induced drain voltage exhibited both the same shape (sinusoidal) and frequency than the gate AC voltage, therefore ensuring that no frequency conversion takes place. The AC amplitude induced in the drain was consistently smaller than the one of the gate's signal (5 mV) as in the sub-THz range the device is unable to amplify signals. The mean value of the induced drain voltage was negative in agreement with the theoretical model [8]. The charge boundary condition for the floating was specified as

$$\oint \vec{D}\overrightarrow{dS} = Q\,, \qquad (1)$$

where $\vec{D}$ is the displacement vector, Q is the total charge and the integral is evaluated over the drain contact surface. Extensive time-domain simulations were conducted for each bias voltage to generate time series to obtain the photovoltaic response of the transistor. Time domain simulations are very time-consuming tasks and state-of-the art multi-core processors need tenths of minutes to obtain the time series of a single bias point. The final calculation of the photovoltaic response from the time series was implemented as a post-processing external to the commercial software.

3 Results and discussions Table 1 summarizes the most relevant DC and AC parameters obtained in simulations. The second row gives the threshold voltage (V_{th}). The third and fourth rows contain the maximum values of the transconductance obtained in simulations (g_m) and in measurements ($g_{m,exp}$), respectively. The differences found in transconductance between measurements and simulations should be attributed to differences in contact resistances and implantations between the simulated transistors and the actual ones.

Table 1 Most relevant DC and AC parameters obtained in simulations.

L_G (nm)	V_{th} (V)	g_m (mS/mm)	$g_{m,exp}$ (mS/mm)	f_T (GHz)
50	-1.2	72	-	36
100	-0.9	98	66	31
250	-0.75	112	76	22
500	-0.675	105	74	11

As the structure of the transistor's gate is a key design parameter to enhance the responsivity of FETs as THz sensors the presented study focused on the effect on device the response of the metal gate variation in length, position and topology (number of fingers).

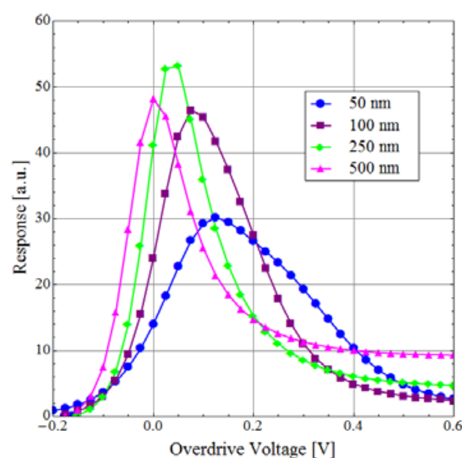

Figure 2 Photovoltaic response of s-Si MODFET with different gate-lengths under THz excitation of 300 GHz vs. gate overdrive.

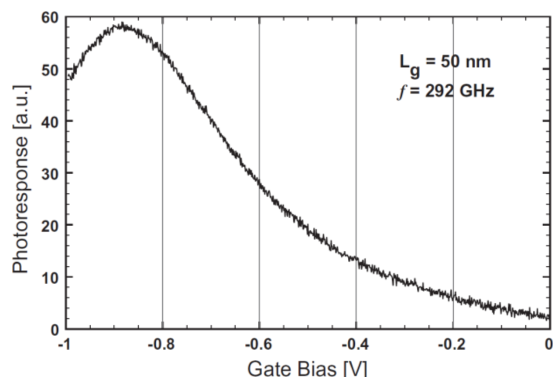

Figure 3 Experimental photovoltaic response of a s-Si MODFET with L_G = 50 nm under THz excitation of 292 GHz [10]. The value of the threshold voltage was V_{th} ≈ -0.84 V.

© 2015 WILEY-VCH Verlag GmbH & Co. KGaA, Weinheim

Figure 2 gives the simulated photovoltaic response of the four simulated transistors when excited at 0.3 THz. Results show a non-resonant response in agreement with theoretical [8] and experimental results (see Fig. 3, [10]). Following the same trend previously obtained in transconductance (Table 1), the THz photovoltaic response is lowered as the gate is shortened owing to a weakened channel control by the gate. The main conclusion to be drawn from Fig. 2 is that neither self-aligned structures, nor very short gate lengths will lead to optimum structures in terms of the THz photoresponse.

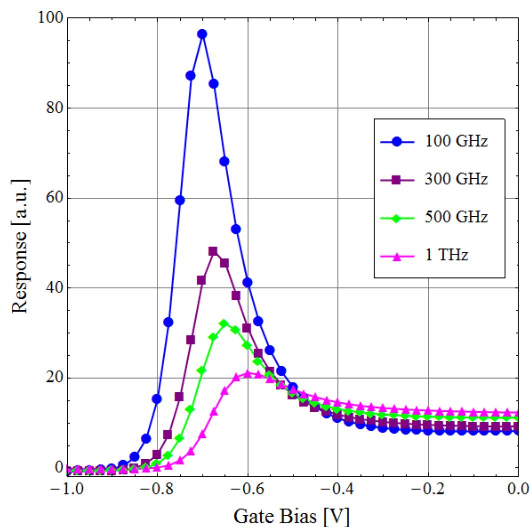

Figure 4 Photovoltaic response of a s-Si MODFET with L_G = 500 nm under THz excitation at different frequencies in the 0.1-1 THz frequency range.

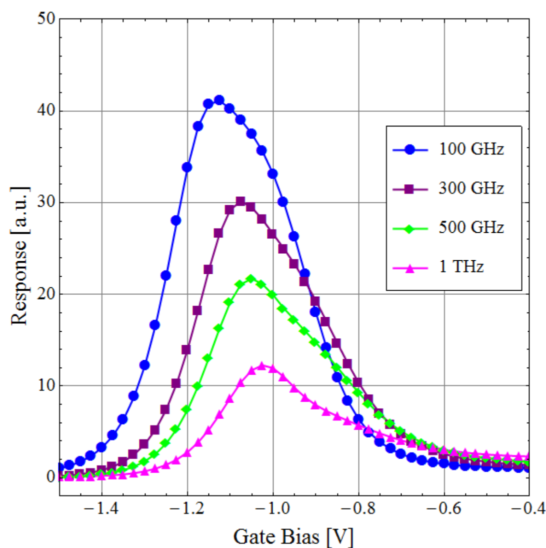

Figure 5 Photovoltaic response of a s-Si MODFET with L_G = 50 nm under THz excitation at different frequencies in the 0.1-1 THz frequency range.

A significant dependence of the photovoltaic response with the excitation frequency was also found in the study. Figures 4 and 5 give, respectively, the photoresponse of the longest and shortest gates in the range considered at four different frequencies between 0.1 and 1 THz. In the full frequency range, the transistor with the longest gate systematically exhibits the best photoresponse. This is in agreement with the above remark: an extreme gate length reduction is detrimental to the device performance as the gate losses control over the channel.

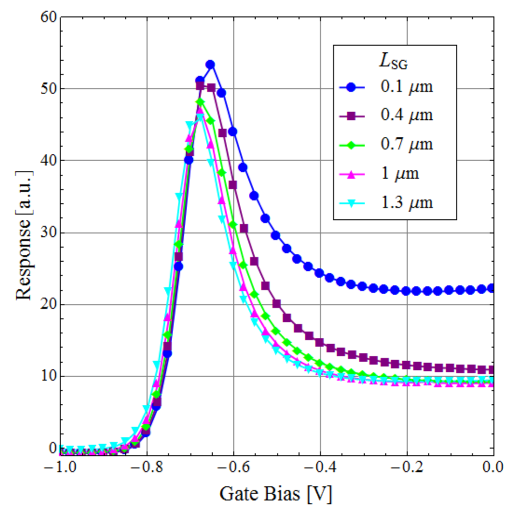

Figure 6 Photovoltaic response of a 500-nm gate transistor placed for four different values of L_{SG} (under a 300 GHz excitation).

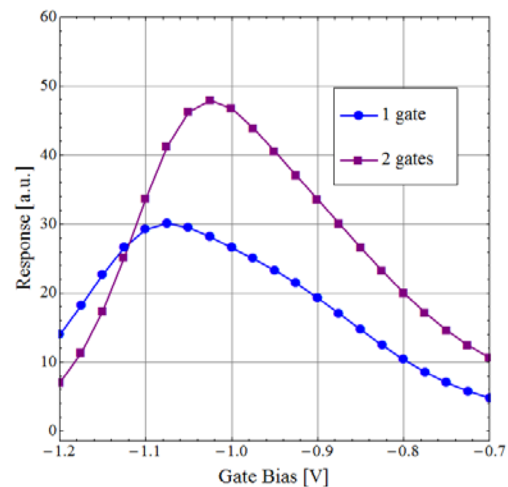

Figure 7 Photovoltaic response of a 50-nm gate transistor for a gate with 1 and 2 fingers equally distributed between source and drain (under a 300 GHz excitation).

Figure 6 gives the photovoltaic response of a 500-nm gate length MODFET when the gate is placed at different distances (L_{SG}) from the source contact: only marginal changes in the photovoltaic response were obtained; in strong

© 2015 WILEY-VCH Verlag GmbH & Co. KGaA, Weinheim

contrast to some commonly accepted ideas, an asymmetric gating of the channel will not necessarily lead to significant enhancements of the THz response. On the contrary, changes of the gate topology, such as a grating of the gate, has a significant impact on the THz photovoltaic response in agreement with FDTD (Finite Differences Time Domain) calculations using a simpler model for the electrons transport in the channel [11]. In Fig. 7 the photovoltaic response of s-Si MODFETs with two configurations of the gate is given: one structure has a conventional single gate (L_G = 50 nm), while a second structure with two gates (actually a gate with two identical 50 nm-fingers) is considered. A large enhancement, roughly 60%, of the photovoltaic response was found in devices with a two-fingers gate as compared to conventional single-finger gate transistors.

4 Conclusions A TCAD study of strained-Si MODFETs is performed to investigate their sub-THz photovoltaic response. To this aim a charge boundary condition for the floating drain contact was implemented. Simulations were performed using a bi-dimensional hydrodynamic model for the charge transport coupled to a Poisson equation solver. In agreement with measurements, a non-resonant sub-THz photovoltaic response is found for the simulated devices. A main result of this study is that the photovoltaic response is strongly influenced by both the gate length and gate topology. As the maximum photovoltaic response changes with both gate length and excitation frequency a careful design of the device is needed to optimize the device parameters (such as its gate length) to obtain a maximum of photovoltaic response In particular, it was found that a dual-finger gate is suitable to obtain better photo-response in the sub-THz range than a conventional single-finger gate.

Acknowledgements This work was supported by the Spanish Ministerio de Economía y Comercio (MINECO) and FEDER under grant # TEC2012-32777.

References

[1] M. Zeuner, T. Hackbarth, M. Enciso-Aguilar, F. Aniel, and H. von Känel, Jpn. J. Appl. Phys. **42,** 2363 (2003).
[2] S. H. Olsen, A. G. O'Neill, L. S. Driscoll, K. S. K. Kwa, S. Chattopadhyay, A. M. Waite, Y. T. Tang, A. G. R. Evans, D. J. Norris, A. G. Cullis, D. J. Paul, and D. J. Robbins, IEEE Trans. Electron Devices **50,** 1961 (2003).
[3] F. Aniel, M. Enciso-Aguilar, L. Giguerre, P. Crozat, R. Adde, T. Mack, U. Seiler, T. Hackbarth, H. J. Herzog, U. König, and B. Raynor, Solid-State Electron. **47,** 283 (2003).
[4] A. Vilches, K. Fobelets, K. Michelakis, S. Despotopoulos, C. Papavassiliou, T. Hackbarth, and U. König, IEE Electron. Lett. **39,** 884 (2003).
[5] Y. M. Meziani, E. García-García, J. E. Velázquez-Pérez, D. Coquillat, N. Dyakonova, W. Knap, I. Grigelionis, and K. Fobelets, Solid-State Electron. **83,** 113 (2013).
[6] K. Fobelets, W. Jeamsaksiri, C. Papavasilliou, T. Vilches, V. Gaspari, J.E. Velazquez-Perez, K. Michelakis, T. Hackbarth, and U. König, Solid-State Electron. **48,** 1401 (2004).
[7] K. Fobelets, W. Jeamsaksiri, C. Papavasilliou, T. Vilches, V. Gaspari, J. E. Velazquez-Perez, K. Michelakis, T. Hackbarth, and U. König, Solid-State Electron. **48,** 1401 (2004).
[8] M. Dyakonov and M. S. Shur, Phys. Rev. Lett. **71**, 2465 (1993).
M. Dyakonov and M. S. Shur, IEEE Trans. Electron Devices **43**, 380 (1996)
[9] Synopsys, Taurus User Guide, Version Z-2007.3, Synopsys Inc., Mountain View, CA, 2007.
[10] Y. M. Meziani, E. García, J. Calvo, E. Diez, E. Velazquez, K. Fobelets, and W. Knap, in: Bolometers, edited by U. Perera (Rijeka, InTech, 2012), chap. 6.
[11] T. Otsuji, V. Popov, W. Knap, Y. M. Meziani, N. Dyakonova, D. Coquillat, F. Teppe, D. Fateev, and J.E. Velazquez-Perez, Japanese Patent PCT/JP2010/007074 (3 December 2010).

© 2015 WILEY-VCH Verlag GmbH & Co. KGaA, Weinheim